RSC Advances

ROYAL SOCIETY OF CHEMISTRY

www.rsc.org/advances

Table of Content Graphic

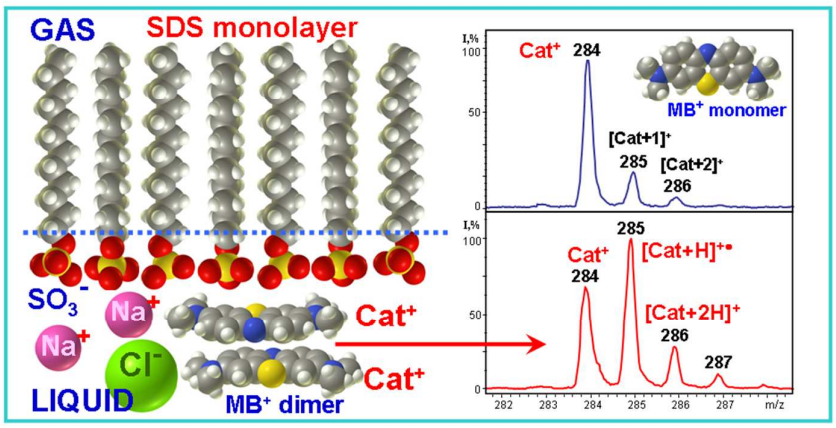

Textual Abstract for Table of Content Entry

Mass spectrometric approach to differentiation of monomer or dimer form of cationic dye methylene blue adsorption at negatively charged nanolayers is proposed. (~20 words)

It is demonstrated that recording of the peak distribution characteristic of the unchanged cation of the dye evidences its monomer form, while observation of reduction products of the dye points to its dimerization or aggregation.

Monomer/dimer dependent modulation of reduction of cationic dye methylene blue in negatively charged nanolayers as revealed by mass spectrometry

Vadim S. Shelkovsky[1], Marina V. Kosevich[1]*, Oleg A. Boryak[1],
Vitaliy V. Chagovets[1], Irina V. Shmigol[2], Valerij A. Pokrovskiy[2]

[1] B.Verkin Institute for Low Temperature Physics and Engineering of the National Academy of Sciences of Ukraine, 47 Lenin Ave., Kharkov, 61103, Ukraine

[2] Chuiko Institute of Surface Chemistry of the National Academy of Sciences of Ukraine, 17, General Naumov str., Kyiv, 03164, Ukraine

Abstract

The possibility to control the reduction rate of redox-active dyes incorporated into nanostructures is of interest for nanotechnology and biomedicine. We propose a novel mass spectrometric approach to study of aggregation-dependent modulation of cationic dye methylene blue (MB) reduction in case of its inclusion into negatively charged nanolayers, which is based on detecting the difference in the redox activity of monomers and dimers of the MB cation (Cat^+). A regular reproducible recording of either intact Cat^+ in case of MB presence in its monomeric form, or one- and two-electron reduction products $[Cat + H]^{+\bullet}$ and $[Cat + 2H]^+$ in case of MB dimers formation, is observed for three different anionic nanostructures with varied content of MB, tested by three mass spectrometric methods: 1) anionic surfactant sodium dodecyl sulfate (SDS) monolayer with adsorbed MB cations at the liquid/gas interface, probed by fast atom bombardment; 2) dried shells of soap bubbles blown from SDS and MB aqueous solution, tested by laser desorption/ionization; 3) a nanotextured surface of porous silicon modified by $-SO_3^-$ groups with adsorbed MB cations, studied by desorption/ionization on silicon technique. The requirement for MB cations to be in the form of dimers or higher aggregates for reduction to be observed under mass spectrometric conditions is justified for the listed systems, where only another MB cation can serve as a source of electron and proton (or hydrogen radical $H^\bullet$) necessary for reduction reaction. The proposed method can be applied to mass spectrometric imaging of stained biological materials, supplying information not only about the localization, but also the MB aggregation state as well.

Key words: Methylene blue dye, SDS, mass spectrometry, reduction, monomers and dimers, nanolayers

Introduction

The present work describes a novel approach to the investigation of the influence of incorporation of a redox-active cationic dye methylene blue (MB) into such soft matter object as a monolayer of anionic surfactant sodium dodecyl sulfate (SDS) on MB redox activity by means of mass spectrometry. The basic idea is that the extent of MB reduction, detectable by mass spectrometry, depends on either monomeric or dimeric form of its inclusion into nanostructures. Three aspects of the problem are considered: characterization of surfactant assemblies doped by the dye, monitoring the modulation of MB redox activity and capabilities of mass spectrometry in these studies.

Self-assembled monolayers of surface active compounds at the liquid-gas interface may be considered as peculiar nano-objects [1] characterized by nano-size in one dimension and micro- or even macro-size in two other dimensions. Incorporation of biologically active compounds into this kind of layer can affect their properties, redox activity in particular [2-5]. Research into reduction processes, i.e. electron and proton transfer, in nanostructures [6-8] which incorporate redox-active organic dyes is of interest for further development of functional nanomaterials and nanodevices.

There is an impressive range of applications of MB dye (**I**) (an organic salt $MB^+ \bullet Cl^-$ or $Cat^+ \bullet Cl^-$). After years of successful application of MB in pharmacology and biomedical research [9-13], in staining and biological imaging [14, 15], its reduction/oxidation properties make it a promising material for nanotechnological applications as a redox indicator and a mediator dye in biosensors [16], as well as a photosensitizer [5] and a component of solar cells materials [17, 18]. To function in such nanomaterials, the MB dye must be immobilized in some carrier or be adsorbed at its surface.

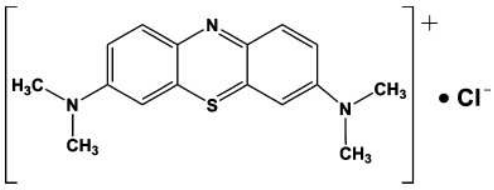

(**I**)

Our mass spectrometric study was stimulated by the reports [3, 4] on the modulation of photochemical properties of MB depending on the form of its adsorption – either monomeric or dimeric - at the negatively charged interfaces of micelles and vesicles formed by the anionic SDS ($An^- \bullet Na^+$) surfactant. It was shown that there can be two scenarios of photochemical processes depending on the aggregation state of MB. When MB^+ cations were mainly in the form of monomers (when SDS is in excess), the mechanism of photochemical transformation of the photoexcited $MB^{+}*$ cation consisted in the energy transfer to molecular oxygen (present in the solution) forming singlet oxygen $^1O_2$. In this case the redox state of the dye did not change.

However, when SDS concentration was low and MB was in excess, $2MB^{2+}$ dimers were more likely to appear; in this case there was electron transfer between the excited and non-excited monomers in the dimer causing the formation of semi-reduced ($MB^{\bullet}$) and the semi-oxidized ($MB^{2+\bullet}$) radicals of MB^{+} [3]. These model experiments were aimed at the clarification of the molecular mechanism of photodynamic therapy of cancer: the negatively charged interface formed by SDS mimicked the membrane of mitochondria as a recognized target for sensitizers, characterized by negative membrane potential [5].

In the cited works [3, 4] methods of fluorescence emission, time-resolved near-infrared emission, absorbance spectroscopy, resonant light scattering, laser flash photolysis and thermal lensing were used. To the best of our knowledge, mass spectrometry had not been applied in order to solve this problem so far. Furthermore, the above mentioned experiments were performed for micelles and vesicles formed in bulk solutions, while mass spectrometry permits to study, as it will be shown below, a surfactant monolayer formed at the liquid-gas interface.

The capabilities of modern mass spectrometry extend far beyond a mere analysis of chemical composition of nanomaterials [19, 20]; there are available studies on noncovalent interactions and *on-line* monitoring of physical and chemical processes [21]. The indisputable advantage of mass spectrometry in the exploration of complex systems is a possibility to record all components of the system simultaneously, which makes it possible to avoid complications characteristic of spectroscopic techniques, caused by band overlap for compounds that are close in structure.

Mass spectrometry can easily identify products of reduction of redox-sensitive dyes by the change in the mass of the analyte. Reduction of various compounds including dyes [22-26], MB [24, 26] in particular, was observed under the condition of various mass spectrometric techniques: secondary ion mass spectrometry (SIMS) and fast atom bombardment (FAB) [22], laser desorption/ionization (LDI) and matrix-assisted LDI (MALDI) [23, 24], and electrospray ionization (ESI) [25].

We have shown recently that the variations in the balance of electrons and protons generated under different mass spectrometric desorption/ionization techniques affect the rate of reduction of heterocyclic dyes [27]. Moreover, mass spectrometry can also monitor the way how the interactions of dyes with their environment influence the reduction rate [28-32]. On this basis we have formulated a mass spectrometric approach to the observation of changes in reduction of dyes in dependence of experimental conditions, aimed at modeling and studying reduction and oxidation processes in nanostructures. This approach was successfully applied to the study of the form of MB adsorption on carbon nanotubes (CNT) surface [32]. Since no reduction products of MB were recorded in the LDI mass spectra of CNT-MB nanocomposite material, it was assumed

that there are no sources of $H^{\bullet}$ in the vicinity of MB^{+} cations adsorbed at the carbon surface, which implies MB^{+} adsorption in the form of the monomers. This assumption as to structure of the nanocomposite was confirmed by molecular dynamics simulation and quantum chemical calculations [32].

As for surface active compounds, their properties are well studied by different mass spectrometric techniques [33-37]. Such nanostructure as a layer of surfactants at the liquid-gas interface can be formed at the surface of liquid glycerol used as a liquid matrix compound in FAB and liquid SIMS (lSIMS) techniques. Although FAB was one of the very first mass spectrometric methods for analysis of biomolecules, it is now replaced by more efficient ESI [38] and MALDI [39], while SIMS remains a powerful tool both in basic studies and industrial analysis of metals, dielectrics and nanomaterials [40, 41]. The charge state of the bombarding agent (either neutral atoms or ions) does not affect significantly the pattern of secondary emission mass spectra of surfactants. It is known that under FAB or lSIMS a bombarding particle excites a sample material to a depth of about 10 nm [33, 40], which correlates with an average thickness of the surfactants layer at the surface of a liquid matrix. Hence surfactants are mainly sputtered from the surface and signals of matrix compound are usually suppressed [33, 34, 37]. Furthermore, it was proved that any other surface inactive compounds present in the liquid solution can be detected in the FAB or lSIMS mass spectra only if they are incorporated into or adsorbed at the surface layer of surfactants and amphiphiles [42]; solutes present in the bulk liquid are "invisible" in the mass spectra of such systems. Recently we have proposed an alternative model of secondary emission mass spectra formation for liquid samples, named "bubble chamber model" [43]. In the framework of this model bombarding particles initiate boiling, i.e. the emergence of tiny bubbles in the superheated liquid analyte. If the surface of the liquid is covered by a surfactant layer, a common soap bubble is blown and the ions of surfactants are sputtered on the bubble burst. Note that ions release on bubbles burst was demonstrated by other techniques as well [44]. Thus, secondary emission mass spectra reflect adequately the composition of the surfactants monolayer at the liquid-vacuum interface. For ionic surfactants it is possible to identify the composition of the double electric layer [37].

Alongside with liquid-gas interfaces, negatively charged ion-exchange monolayers can be formed at the solid surfaces of nanomaterials, porous silicon in particular [31]. This nanotextured material can be probed by LDI mass spectrometry; LDI involving silicon substrate (target) is referred to as desorption/ionization on silicon (DIOS) or porous silicon [45, 46]. Solid surface of porous silicon functionalized by $–SO_3^-$ groups can mimic immobilized layer of $–SO_3^-$ polar heads of SDS.

The above mentioned experience enabled us to formulate the task which is to develop an approach to mass spectrometric investigation of MB dye redox activity modulation depending on the peculiarities of its adsorption at negatively charged liquid-vacuum and solid-vacuum interfaces. The idea to be verified is rather simple: it is expected to observe the reduction of MB in the systems where MB^+ is in dimeric (aggregated) form and absence (or dramatic suppression) of reduction for the systems with the dominance of MB^+ monomers.

Experimental

FAB mass spectrometric measurements were performed using magnetic sector mass spectrometer MI-1201E ('SELMI' Works, Sumy, Ukraine) equipped with commercial FAB primary and secondary ion sources. Argon was used as a bombarding gas; the energy of the primary beam was 4.5 keV.

Samples for FAB measurements were prepared by mixing of equal volumes of glycerol, used as a viscous liquid FAB matrix, and water solution of the mixture of MB and SDS. 5 μL drop of the liquid was deposited onto a standard sample holder and introduced into the secondary ion source through direct inlet system. Water co-solvent was evaporated under fore-vacuum conditions in the inlet chamber leaving the concentration of the components in glycerol the same as in the initial water solution [37]. Surfactant monolayer as the main object of study was spontaneously formed at the liquid-vacuum interface. MB and SDS were taken in different ratios to provide varied conditions for MB^+ adsorption at the SDS layer. In order to avoid micelles formation but, at the same time, to obtain detectable signal of SDS, the lowest SDS concentration was below critical micelle concentration (c.m.c. $8 \cdot 10^{-3}$ M [47]); whereas the highest concentration was 10^{-1} M. The MB concentration ranged from 10^{-4} M to 10^{-2} M. Mass spectral patterns obtained for at least three independent depositions of fresh samples with each components ratio showed good reproducibility; the scattering of peaks intensities from measurement to measurement did not exceed 3-5% in average.

LDI and DIOS experiments were performed with the help of Autoflex II mass spectrometer (Bruker Daltonics, Germany) equipped with a nitrogen laser (λ = 337 nm). The desorption/ ionization was performed by laser pulses of 3 ns length and 20 Hz frequency. The delayed extraction time was set to 30 ns. The acceleration voltage was 20 kV. Spectra were recorded by summing up 100 laser shots.

A special method was applied to prepare samples for LDI measurements. Foam was whipped up from the water solutions of SDS-MB mixtures; thus formed soap bubbles were transfered onto a standard metal sample holder, where they burst and dried. Since MB absorbs UV light, there is no need in any organic matrix used in UV MALDI [39], which permits to probe MB-

SDS system by LDI without any additives. Water solutions of (SDS+MB) were the same, as those used in the FAB experiments. Reproducible LDI mass spectral patterns were obtained for three independent depositions of each sample.

Pure MB was deposited onto the metal sample holder or porous silicon wafer from water solution using a standard dry drop method.

The substrate for DIOS measurements – porous silicon (PS) functionalized by ion-exchange $-SO_3H$ groups (PS-SO_3H) – was prepared as described earlier [31, 48]. The adsorption of MB^+ at the PS-SO_3H surface of the silicon wafer was performed from 10^{-4} M MB solution in ethanol during 2 hours. The silicon wafer extracted from the solution was dried and fixed at the metal sample plate.

The commercial sources of the reagents were as follows: MB dye ("Reachim", Moscow, the Russian Federation), SDS ("Serva", r.g., Heidelberg, Germany), glycerol ("Sigma", ≥ 99%, Steinheim, Germany). Deionized water was used to prepare the solutions.

Results and discussion

In order to reveal the effect of MB cations adsorption at anionic layers on MB redox activity, three systems were examined by three mass spectrometric techniques.

1) The monolayer formed at the surface of glycerol solution of SDS anionic surfactant with MB inclusion was probed by particle bombardment under FAB conditions.

2) Dried shells of soap bubbles blown from SDS and MB solution in water were affected by UV laser pulsed irradiation under LDI conditions.

3) MB adsorbed on the surface of porous silicon modified by ion-exchange $-SO_3H$ groups was studied by UV LDI (referred to as DIOS method).

1. *Basic principles of mass spectrometric study of reduction process*

Reduction usually does not occur spontaneously in the media chosen for samples preparation for mass spectrometry, such as glycerol matrix for FAB, organic matrices for MALDI, or organic solvents in ESI. The reduction is initiated by the impact of ionizing agents used in mass spectrometric experiments. The initiating role of ionizing agents lies in the generation of free electrons and protons (or $H^\bullet$ radicals) necessary for reduction of the dyes. The sources of protons and electrons are dyes molecules themselves and/or the surrounding medium.

Reduction of redox-active cationic dyes, including MB ($Cat^+ \bullet Cl^-$), proceeds in two stages. Semi-reduced cation radical is formed in one-electron process:

$$Cat^+ + e^- + H^+ \rightarrow (Cat^\bullet + H^+) \rightarrow [Cat + H]^{+\bullet} \quad \text{or} \qquad (1)$$

$Cat^+ + (e^- + H^+) = (Cat^+ + H^\bullet) \rightarrow [Cat + H]^{+\bullet}$ (1')

Complete two-electron reduction produces a neutral product:

$Cat^+ + 2e^- + H^+$ or $[Cat + H]^{+\bullet} + e^- \rightarrow (Cat + H)^o$ (2)

Note, that only charged species (shown here in brackets) can be detected by mass spectrometry. Charged product $[Cat + H]^{+\bullet}$ of the reactions (1), (1') can be directly detected in the mass spectra alongside with the initial cation Cat^+. Neutral product of reaction (2) is detected in the protonated form:

$(Cat + H)^o + H^+ \rightarrow [Cat + 2H]^+$ (3)

It should be noted that the isotopic yield (mainly due to ^{13}C) must be subtracted from the intensity of peaks at (Cat + 1) and (Cat + 2) masses to determine actual contribution of the reduction products. The isotopic distribution calculated for the MB cation peaks group Cat^+ : (Cat + 1) : (Cat + 2) is as follows 100 : 20 : 6.

If MB^+ dimers are present in the system probed by FAB/lSIMS, the excitation of $2MB^{2+}$ can occur due to the fact that a secondary electron generated by primary bombarding particles is trapped:

$(2Cat)^{2+} + e^- \rightarrow (2Cat)^{+\bullet}$ (4)

A pathway of dissociation of the odd-electron dimer can lead to the formation of the semi-reduced product:

$(2Cat)^{+\bullet} \rightarrow [Cat + H]^{+\bullet} + [Cat - H]^o$ (5)

Further transformations of $[Cat + H]^{+\bullet}$ may proceed in accordance with reactions (2) and (3).

2. ***(SDS + MB) system probed by FAB mass spectrometry***

A soft matter nano-object, i.e. a monolayer of anionic surfactant SDS, which incorporates MB^+ cations, is spontaneously formed at the surface of (SDS + MB) solution in liquid glycerol. Fig. 1a shows a schematic representation of the double electric layer formed by SDS anions balanced by Na^+ counterions at the liquid-gas interface. Adsorbed MB^+ cations replace sodium cations in this layer. An evaluative comparison of the sizes of SO_3^- polar head groups of SDS and MB^+ cation (Fig. 1b) demonstrates that the area covered by the cation matches the area occupied by two SO_3^- groups. This may be a mechanistic reason which facilitates dimerization of adsorbed MB^+ cations to compensate the charge of two displaced Na^+ counterions.

It was shown earlier that a relatively low concentration of a surfactant (about 10^{-5} M) is sufficient for complete coverage of the surface of a glycerol droplet under FAB/lSIMS conditions [33]; further increase of the bulk concentration of the surfactant up to and above its critical micelle concentration ($8 \cdot 10^{-3}$ M for SDS [47]) does not affect the mass spectra of the matter sputtered from the thin surface layer. On the other hand, MB concentration influences the

way it binds to the negatively charged surface layer, since the MB to SDS ratio affects the partition of MB between the surface layer and micelles formed in the bulk solution [2, 3].

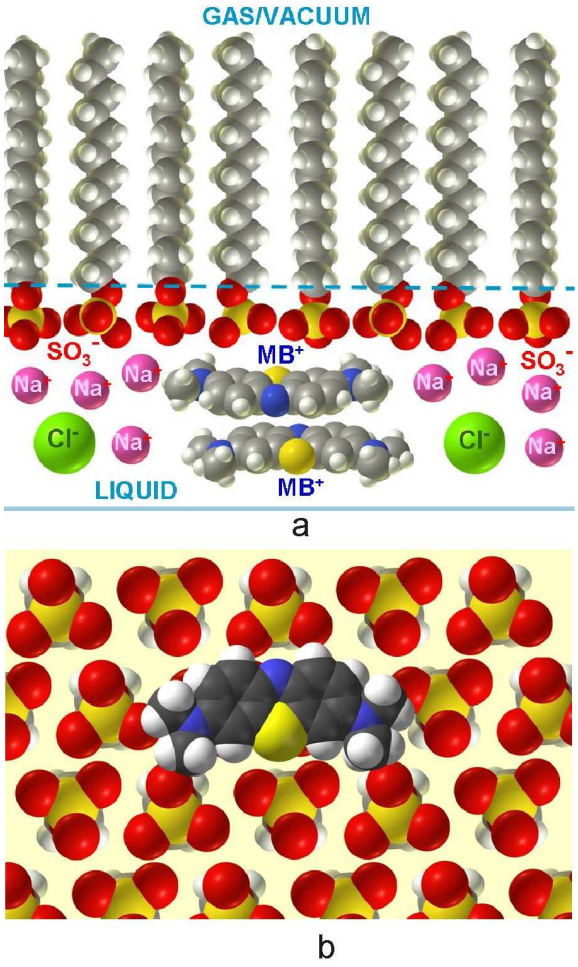

Fig. 1. Schematic representation of (SDS + MB) system at the liquid-gas interface: a) double electric layer formed by SDS anions and Na^+ counterions with inclusion of $2MB^{2+}$ dimer; b) orthogonal view of arrangement the SO_3^- polar heads of SDS with adsorbed MB^+ cation. (Colour scheme for atoms: hydrogen – white, carbon – grey or dark grey, nitrogen – blue, oxygen – red, sulfur – yellow, chlorine – green, sodium – magenta.)

Positive ion FAB mass spectra of the individual components of the system under study, namely MB and SDS, are already well known. Anionic surfactant SDS ($An^-•Na^+$) is characterized by a set of organic anion-sodium counterion clusters $nAn^-•(n+1)Na^+$ (n = 1, *m/z* 311; n=2, *m/z* 599; n=3, *m/z* 887) that become less abundant as n increases [37]. As for MB, reduction is usually observed for its solutions in glycerol under FAB. Typical FAB mass spectrum of MB sputtered from its solution in the glycerol matrix (Fig. 2a) is represented by a group of peaks, which includes the first monoisotopic peak of organic cation of the dye Cat^+, *m/z* 284 (which relative intensity is assumed to be 100%) and a number of satellite peaks. The intensity of the second peak at *m/z* 285 (164%) is comprised by 20% of isotopic contribution of

the cation and 144% yield of the semi-reduced product of reaction (1) - $[Cat + H]^{+\bullet}$. The third peak at *m/z* 286 contains 26% contribution of the protonated reduction product of reaction (3) - $[Cat + 2H]^{+}$, obtained after the subtraction of the yields of the third isotopic peak of Cat^{+} (6%) and the second isotopic peak of $[Cat + H]^{+\bullet}$ (29%). As a result, the whole amount of MB (100%) is represented by 37% of the intact dye, 53% of the semi-reduced product and 10% of the two-electron reduction product in the FAB mass spectrum.

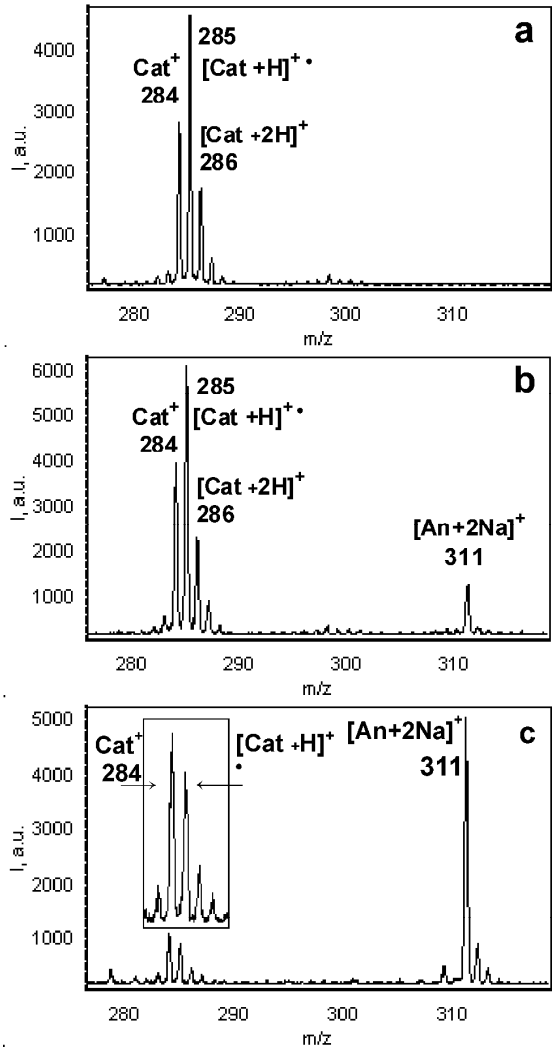

Fig. 2. FAB mass spectra of the surface layer of (SDS + MB) system in glycerol matrix:
a) pure MB (10^{-2} M) without SDS;
b) a mixture of 10^{-1} M SDS and 10^{-2} M MB;
c) a mixture of 10^{-1} M SDS and 10^{-4} M MB.

It should be noted that on FAB sputtering of the surface of true solution of MB in glycerol, it is hard to separate the contribution of excited species generated by particle bombardment from either MB^{+} dimers (aggregates) or glycerol solvent molecules [22, 26] to the total outcome of

reduction of MB^+. In the case of glycerol surface coverage by ionic surfactants, glycerol molecules adjacent to the surface double electric layer, as it was proved earlier [37], are strongly bound with the counterions of the surfactant salt (Na^+ for SDS), which together with the limited content of glycerol in the sputtered volume [37, 42] prevents noticeable participation of glycerol-related species in the bombardment-initiated redox reactions.

The (SDS + MB) systems with different ratios of MB to SDS in glycerol were tested. Representative FAB mass spectra of two samples with SDS bulk concentration of 10^{-1} M and relatively high (10^{-2} M) or relatively low (10^{-4} M) concentrations of MB are shown in Fig. 2b and Fig. 2c, respectively. The mass spectra contain peak envelopes characteristic of the both components of the system. It should be noted here that the recording of MB signals proves the inclusion of the cation of the dye into the surface double electric layer.

The main point of interest is to understand how mass spectral pattern of the (SDS + MB) system depends on MB concentration. It can be seen that at relatively high MB content (Fig. 2b) the peaks evidencing the reduction of the MB^+ cation are intense; the relative yields of the reduction products are practically the same as in the case of concentrated solution of neat MB (Fig. 2a). At relatively low concentration of MB rather small deviation from the isotopic distribution is observed in the Cat^+ peaks group (Fig. 2c), which points to very low rate of the MB reduction.

The observed differences in FAB mass spectral patterns point to different forms of adsorption of MB^+ cations at the negative surface layer of SDS anions, which can be either monomeric or dimeric depending on the MB content in the system. The underlying mechanisms of secondary ion mass spectra formation are the following. Secondary electrons to be trapped by the redox-active MB^+ are generated in any system by the primary particles impact. The electron scavenging by a single MB^+ cation produces neutral species. A proton H^+ (or, alternatively, $H^\bullet$ radical) is required to produce the charged product of reactions (1) or (1'), detected by mass spectrometry. In the case of MB^+ adsorption at the SDS layer in the form of separate monomers, there is no source of H^+ or $H^\bullet$ radicals to be generated under FAB in the surrounding of a single MB^+, comprised by SO_3^- head groups of SDS and Na^+ counterions in the double electric layer (Fig. 1). Thus, there are no "reagents" for MB^+ reduction reaction to be completed (Fig. 2c). In the case of MB^+ adsorption at SDS layer in the form of dimers (aggregates), a monomer within the dimer excited by trapping a secondary electron $(2Cat)^{+\bullet}$ (4) can serve as a source of $H^\bullet$ radical to complete one-electron reduction of another MB^+ monomer (5) (Fig. 2b).

It should be noted that the "overdraft" of the peaks at *m/z* 285, 286 caused by MB reduction products persists down to rather low MB content in the system as MB concentration decreases, which means that dimers are assembled near the negatively charged SDS anions layer in a wide

range of MB bulk concentrations. Even at 10^{-4} M MB concentration the reduction is not suppressed completely (Fig. 2c). Tests at lower MB concentrations do not meet the sensitivity limit for reliable detection of MB signals. Note that the excessive concentration of SDS in comparison to that required for the surface monolayer formation helps to engage some amount of MB^+ in binding to SDS micelles in the bulk liquid, which reduces the amount of MB^+ available for binding to the surface layer.

MB^+ cations adsorption at the SDS anions by replacement of Na^+ counterions in the surface double electric layer, as shown in Fig. 1a, finds support in the FAB mass spectral pattern as well. Namely, although the filling of the surface by SDS anions must be the same in the samples with the same SDS content, the absolute abundance of SDS-related clusters $An^-•2Na^+$ is much lower for the sample with high MB content (Fig. 2b) than for the sample with low MB content (Fig. 2c). The obvious reason is the depletion of Na^+ content, required for $An^-•2Na^+$ clusters formation, in the surface layer enriched by MB^+ cations. Larger clusters $nAn^-•(n+1)Na^+$ with $n>1$ are suppressed in the mass spectra as well. Similar clusters of SDS anion An^- with two MB^+ cations or mixed Na^+ and Cat^+ cations are, obviously, unstable in the gas phase, since they were not detected in the FAB mass spectra.

It is of interest to estimate the efficiency of the MB^+ cations adsorption at the SDS surface monolayer, that is the difference between the preset molar ratio of the components in the initial solution and the components ratio in the matter sputtered from the surface of the sample. The direct transfer to the gas phase of the so-called “preformed” or “performed” ions of the dissociated ionic compounds under desorption mass spectrometric conditions permit to avoid ambiguities caused by differences in ionization potentials characteristic of neutral compounds. Thus, evaluation of the ratio of ionic species in the system on the base of their peak intensities (ion currents) in the mass spectra seems reasonable. However, there are certain problems for (SDS + MB) system connected with the necessity of proper account of contribution of MB^+ reduction products and peculiarities of the clustering of SDS anions with sodium counterions, cased by the substitution of some share of Na^+ by MB^+ cations in the surface layer. Rough estimates made with account of these factors, described in the “Electronic Supplementary Information”, show that the ratio of MB to SDS derived from the mass spectra is higher than the initial molar ratio of the components, which evidences in favour of MB^+ adsorption at the surface SDS layer.

Similar results can be expected from the measurements with instruments operating in SIMS mode, since literature data [22, 26, 37, 42] show good qualitative agreement of mass spectral patterns of ionic compounds obtained both under FAB and liquid SIMS conditions.

3. ***(SDS + MB) system under LDI mass spectrometry***

Soap bubbles blown from aqueous solution of SDS with MB were dried on the metal sample holder, as described in the "Experimental". The structure of the soap bubbles walls is destroyed in the process of drying and solidification, but the ratio of the components is preserved in the dried shells.

The main ions in the LDI mass spectra of the individual components are similar to those observed under FAB. There is an abundant cluster $An^{-}•2Na^{+}$, *m/z* 311, and Na^{+} ion in the positive ion mass spectrum of SDS. Reduction related peaks are observed in the LDI and MALDI mass spectra of MB [24]; the ratio of the peaks in the cation peaks group depends, however, on the type of substrate and ionization parameters [30-32]. The extent of reduction of microcrystalline MB under LDI from bare metal substrate (Fig. 3a) is similar to that observed under FAB for neat MB (Fig. 2a).

Fig. 3b,c presents LDI mass spectra of two (SDS + MB) systems with the same ratios of the components in aqueous solution as in FAB experiments described before. It can be seen that at high MB content (Fig. 3b) peaks corresponding the semi-reduced product $[Cat + H]^{+•}$ (1) and protonated two-electron reduction product $[Cat + 2H]^{+}$ (3) are rather high. At low MB content (Fig. 3c) the main peak in the MB group is that of the cation Cat^{+}, *m/z* 284, and the reduction is practically absent.

Thus, the effect of the suppression of reduction at low MB content and excessive SDS is reproduced under LDI similarly to FAB, in spite of certain distinctions in mechanisms of ions production under two ionization techniques and different aggregate states of the samples. Under LDI/MALDI conditions ions formation takes place in ion-molecule reactions in the plume of material evaporated or ablated by a laser shot [39, 49]. The reactive species necessary for the formation of certain types of ionic products must be present in the plume. The sample with high content of MB creates a reactive mixture where reactions (1)-(5) between MB^{+} cations or dimers and electrons, protons or hydrogen radicals generated by a laser shot result in the reduction of some part of MB (Fig. 3a,b). Electrons are supplied to the plume either from the sample material or from the metal sample holder [50]. The protons or hydrogen radicals appear in the plume due to dissociation of excited MB cations (or their dimers and higher aggregates). There is an obvious lack of protons in the plume generated from the sample with very low MB content, which is the limiting factor for completion of reduction of MB^{+} cations (Fig. 3c).

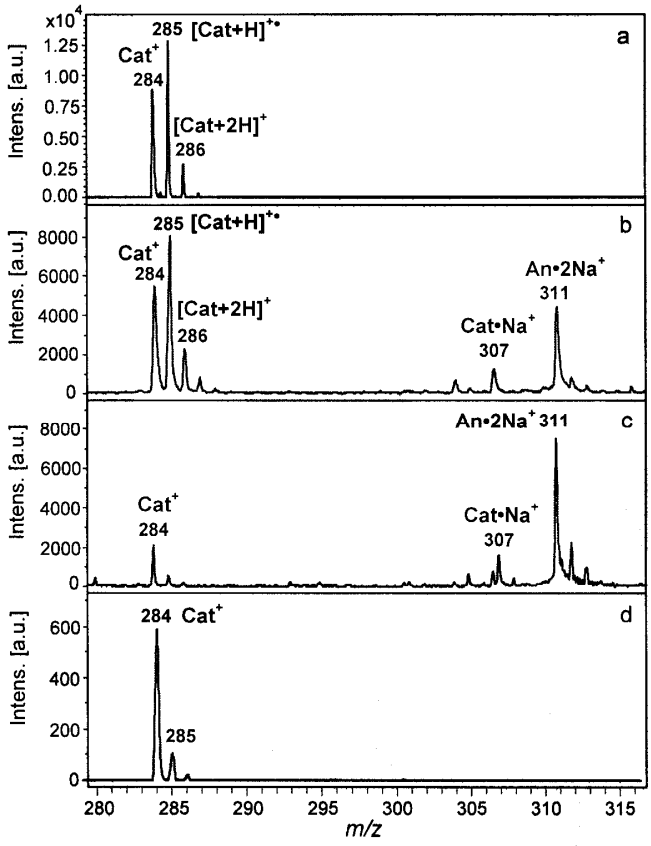

Fig. 3. LDI mass spectra of MB and (SDS + MB) systems: a) pure crystalline MB; b) a mixture of 10^{-2} M MB and 10^{-1} M SDS; c) a mixture of 10^{-4} M MB and 10^{-1} M SDS; d) LDI (DIOS) of MB adsorbed on PS-SO_3^- ion-exchange surface.

A mechanism connected with UV irradiation interaction with a solid sample should be considered for LDI conditions as well. The process of UV light absorption by solid MB, described in the early work [51], results in the formation of semi-reduced and semi-oxidized species due to electron transfer between the neighboring cations:

$$2Cat^{2+} + h\nu \rightarrow 2Cat^{2+}* \rightarrow Cat^{\bullet} + Cat^{2+\bullet} \qquad (6)$$

Under LDI this "laser ionization" event is closely followed by the "laser desorption" step. Once the products of the reaction (6) are transferred to the plume, $Cat^{\bullet}$ can encounter H^+ as in reaction (1), and $Cat^{2+\bullet}$ can trap an electron transforming back to Cat^+.

There is a peak at *m/z* 307 in the LDI mass spectra of (SDS + MB) systems, absent in the FAB mass spectra, which may help to clarify some mechanisms of ion formation under LDI. Either the reaction (6) or a step of electron capture by a single MB^+ cation (7) in the plume produces a reactive radical $Cat^{\bullet}$

$$Cat^+ + e^- \rightarrow Cat^{\bullet}\ , \qquad (7)$$

which can attract a proton as in reaction (1), that is to be protonated. Another abundant pathway of "ionization" of neutrals under LDI and MALDI, however, is the so-called "cationization", i.e.

attachment of alkali metal ions [39]. Since there is a plenty of Na^+ ions originating from SDS in the plume, the following cationization reaction is possible:

$$Cat^{\bullet} + Na^+ \rightarrow Cat^{\bullet}{\bullet}Na^+ \quad (8)$$

The abundance of $Cat^{\bullet}{\bullet}Na^+$ ion is comparable with that of Cat^+ for the system with SDS excess (Fig. 3c). This means that despite electron capture by Cat^+ (7), as it was predicted above, there is a lack of protons to complete the reaction (1) via protonation of $Cat^{\bullet}$, which results in its cationization by Na^+ being in excess instead. On the other hand, the abundance of $Cat^{\bullet}{\bullet}Na^+$ ion is relatively low for a system with MB excess (Fig. 3b), where protons are readily available for reaction (1). The occurrence of the reaction (8) demonstrates that separate steps of electron capture followed by either H^+ or Na^+ attachment can be realized under LDI. The reaction (8) does not occur under FAB since a limited number of Na^+ cations present in the surface layer enriched by MB^+ can participate in bombardment-initiated reactions; at the same time the whole amount of Na^+ of the solid SDS salt is transferred to the reactive plume under LDI.

The question arises if it is possible to monitor a signal of $(2MB)^{2+}$ dimer directly. There are several reasons hampering $2MB^{2+}$ observation. The main reason is the coincidence of *m/z* (where *z* is the charge) values of singly charged monomer and doubly charged dimer. The odd value of the first isotopic peak of the dimer (*m/z* = (284+285)/2), however, can be observed at a fractional mass value. Indeed, the LDI mass spectrum of crystalline MB recorded in reflectron mode shows very small peak at *m/z* 284.5 (Fig. 3a). It proves the survival of a small share of $2MB^{2+}$ dimers under LDI in the gas phase; this kind of peak is never observed in the group of peaks of the single unreduced cation. The abundance of such isotopic peak, however, is too small for reliable detection of the dimers. Secondly, in contrast to ESI, multiply charged ions are rarely observed in desorption techniques. Doubly charged ions sputtered to the gas phase are usually destabilized by coulombic repulsion between the charged sites. Not only noncovalent associates, but also molecular ions, e. g. dications of bisquaternary ammonium compounds, tend to avoid doubly charged state by the so called charge separation reactions [52, 53].

Thus, in spite of certain differences between some mechanisms of gas-phase (in-plume) reactions under LDI of solid samples and sputtering of the surface film under FAB, the reason why MB reduction products are present or absent is still the same. Namely, the content of MB in the mixture with anionic surfactant, sufficient for contacts and interactions between MB^+ cations, is a necessary prerequisite for MB reduction.

4. *LDI of MB on modified porous silicon*

In order to continue the verification of the effects of negatively charged media on MB reduction, LDI/DIOS was used to probe MB adsorbed on the surface of solid porous silicon

modified by ion-exchange $-SO_3^-$ groups ($PS-SO_3H$) (Fig. 3d). It can be assumed, that the surface layer of $-SO_3^-$ groups mimics the arrangement of $-SO_3^-$ polar heads of the SDS interfacial layer.

The adsorption of MB^+ cations at the $PS-SO_3H$ surface proceeds by ion-exchange mechanism [31]:

$$PS-SO_3H + Cat^+ \bullet Cl^- \rightarrow PS-SO_3^- \bullet Cat^+ + HCl \quad (9)$$

A monolayer of salt-like species $PS-SO_3^- \bullet Cat^+$ is obviously formed at the surface. The LDI mass spectrum produced from this surface contains a group of peaks of MB^+ with the isotopic distribution characteristic of the unmodified cation alone (Fig. 3d). Obviously, the desorption of single, the so called "preformed", MB^+ cations proceeds together with thermal dissociation of the salt-like species under DIOS conditions.

Note that the product of reaction (7) at *m/z* 307, characteristic of LDI of (SDS + MB) mixtures at the metal substrate, is absent in the DIOS mass spectrum of MB^+ adsorbed at the $PS-SO_3H$ surface, which agrees with the absence of sodium cations in this system.

Certain differences between LDI/DIOS mass spectral pattern of MB deposited onto unmodified and modified porous silicon were observed [31]. MB solution drying at the neat porous silicon surface obviously causes the formation of aggregates or small crystals of MB in the cavities at the nanostructured surface. DIOS mass spectra of MB in this case practically coincide with its LDI mass spectra obtained from the metal sample holder (Fig. 3a), meaning that they contain reduction products.

It can be summarized that peaks envelope characteristic of the intact MB^+ cation as a marker of its monomeric form in the system under study was observed for negatively charged soft matter monolayer of SDS anions with very low content of adsorbed MB^+, assembled at the liquid-gas interface (Fig. 2c); solid SDS films with low content of MB (Fig. 3c); MB^+ adsorbed at the $-SO_3^-$ monolayer immobilized on porous silicon surface (Fig. 3d), and, earlier, for carbon nanotubes-MB nanocomposite [32]. Abundant reduction products $[Cat + H]^{+\bullet}$ and $[Cat + 2H]^+$ were reproducibly recorded in the desorption mass spectra of the systems, where dimerization or aggregation (up to crystallization) of MB was possible: concentrated solution of MB (Fig. 2a), microcrystalline MB salt on the metal (Fig. 3a) or porous silicon [31] substrates; SDS interfacial monolayers with high content of MB (Fig. 2b) and solid SDS films with high MB content (Fig. 3b).

5. Implications

The obtained results demonstrate that desorption/ionization mass spectrometric techniques can be added to the arsenal of tools for monitoring of interactions of MB, its dimerization and reduction in complex media.

Monitoring changes in the aggregation state of the MB dye at negatively charged interfaces is currently harnessed in the research of some biological processes on molecular level. As it was already mentioned in the Introduction, monomeric or dimeric form of adsorption of MB^+ at the negatively charged mitochondria membrane alters the type of mechanism responsible for photodynamic therapy of cancer [3-5]. In the course of development of DNA hybridization sensors [54] certain differences in MB^+ binding to single- and double-stranded DNA molecules immobilized on some carrier were observed. Single MB^+ cations bind electrostatically with negatively charged phosphate groups of single-stranded DNA. Intercalation of MB^+ cations into double-stranded DNA made it possible to observe the reduction of MB^+. In this case MB^+ reduction was promoted by the stacking interactions of MB^+ with heterocyclic nitrogen bases of DNA, rather than by its dimerization. The relationship between the dimerization constants of MB and its bactericidal activity was studied [55]. Dimer-monomer transition of MB^+ is utilized in development of an enzyme-specific activatable probe using photoacoustic imaging [56]. Transition from the monomers to dimers of MB^+ was observed on gel-to-liquid crystalline phase transition in telomere-bilayer membranes [57]. Synthesis of photosensitizing nanoparticles with a specified ratio of monomers to dimers of phenothiazine photosensitizers, designed for modulation of production of singlet oxygen vs radical species in photo-induced processes, was reported [58].

Currently there is a rapid development of imaging mass spectrometry of biological objects by both SIMS [59, 60] and LDI/MALDI [15, 60-62]. The main customers of new imaging techniques are oncologists looking for molecular biomarkers for more reliable cancer diagnostics [15, 61-63]. Since MB is used for staining biological material, the same stained tissue sample can be imaged by the combination of spectroscopic and mass spectrometric techniques. The mass spectral features of MB revealed in the present work can be applied for more deep interpretation of imaging results. Namely, the dominance of the peak of the intact cation at *m/z* 284 in certain imaged sites may indicate the adsorption of single cations at the negatively charged moieties of biomolecules or biomembranes. Alternatively, the dominance of the reduction product at *m/z* 285 may testify to the aggregation of MB molecules in some nano-cavities of the biopolymers, cells or tissues.

Conclusions

The present paper proves the substantiality of the mass spectrometry-based approach to monitoring the aggregation-dependent modulation of cationic dye MB reduction in negatively charged nanostructures. Generally, the proposed method is rather simple: observation of the peak distribution characteristic of the unchanged cation of MB in desorption mass spectra of any MB-

containing system indicates MB^+ monomeric distribution in the surrounding medium, whereas observation of reduction products of MB^+ ($[Cat + H]^{+\bullet}$ and $[Cat + 2H]^+$) testifies to its dimerization (aggregation). This effect can be detected by a number of mass spectrometric techniques, such as FAB, lSIMS, LDI, DIOS. These observations correlate with available spectroscopic data for similar systems with varied MB monomer/dimer ratio [3, 4]. At the same time, while spectroscopic data are related mainly to micelles or aggregates in the bulk solution, desorption mass spectrometry permits to probe thin surface layers and films, including self-assembled monolayer of surfactants at the liquid-gas interface.

The paper suggests a basic explanation of the difference in mass spectral patterns of the monomers and dimers of MB adsorbed at the negatively charged surface. The presence of several MB^+ cations being in close contact is required for generation and transfer of both electron and proton (or hydrogen radical $H^\bullet$) during desorption/ionization events under mass spectrometric conditions. Absence of any species which can serve as a source of hydrogen radicals required for the reduction of a single MB^+ cation at the SDS layers or at the PS-SO_3^- surfaces prevents reduction and prompts direct desorption of the intact preformed Cat^+.

A revealed possibility to control redox activity of MB by providing conditions for the formation of its either monomer or dimer form in the anionic nanolayers may be used in the elaboration of nanomaterials and nanodevices. The monomer/dimer dependence of mass spectral pattern of MB may be used in the interpretation of data provided by mass spectrometric imaging of MB-stained biological material.

Acknowledgements. This work was partially supported by research grant N 37/14-nano of the National Academy of Sciences of Ukraine.

References

1. Nanostructured soft matter: experiment, theory, simulation and perspectives (NanoScience and Technology), ed. A. V. Zvelindovsky, Springer, 2007, 628 p.
2. M. K. Carroll, M. A. Unger, A. M. Leach, M. J. Morris, C. M. Ingersoll and F. V. Bright, *Appl. Spectrosc.,* 1999, **53**, 780-784.
3. H. C. Junqueira, D. Severino, L. G. Dias, M. S. Gugliotti and M. S. Baptista, *Phys. Chem. Chem. Phys.,* 2002, **4**, 2320–2328.
4. D. Severino, H. C. Junqueira, M. Gugliotti, D. S. Gabrielli and M. S. Baptista, *Photochem. Photobiol.,* 2003, **77**, 459–468.
5. D. Gabrielli, E. Belisle, D. Severino, A. J. Kowaltowski and M. S. Baptista, *Photochem. Photobiol.,* 2004, **79**, 227–232.
6. G. Gilardi and A. Fantuzzi, *Trends Biotechnol*., 2001,**19**, 468–476.
7. V. M. Rotello, *Curr. Org. Chem.,* 2001, **5**, 1079–1090.
8. O. Azzaroni, M. Álvarez, A. I. Abou-Kandil, B. Yameen and W. Knoll, *Adv. Funct. Mater.,* 2008, **18**, 3487–3496.
9. R. H. Schirmer, H. Adler, M. Pickhardt and E. Mandelkow, *Neurobiol Aging.,* 2011, **32**, 2325.e7–2325.e16.
10. S. Scheindlin, *Mol. Interventions,* 2008, **8**, 268–273.
11. J. II Clifton and J. B. Leikin, *Am. J. Therapeut.,* 2003, **10**, 289–291.
12. (a) J. E. Kristiansen, *Dan. Med. Bull*., 1989, **36**, 178–185.
(b) P. R. Ginimuge and S. D. Jyothi, *J. Anaesthesiol., Clin. Pharmacol.,* 2010, **26**, P. 517–520.
(c) R. H. Schirmer, B. Coulibaly, A. Stich, M. Scheiwein, H. Merkle, J. Eubel, K. Becker, H. Becher, O. Müller, T. Zich, W. Schiek and B. Kouyaté, *Redox Rep.,* 2003, **8**, 272–275.
13. (a) M. Wainwright and L. Amaral, *Trop. Med. Int. Health*., 2005, **10**, 501–511.
(b) M. J. Ohlow and B.Moosmann, *Drug Discovery Today,* 2011, **16**, 119–131.
14. J. Mérian, J. Gravier, F. Navarro and I. Texier, *Molecules,* 2012, **17**, 5564–5591.
15. P. Chaurand, S. A. Schwartz, D. Billheimer, B. J. Xu, A. Crecelius and R. M. Caprioli, *Anal. Chem.,* 2004, **76**, 1145–1155.
16. (a) X. Wu, T. Ying and K. Sun, *J. Shanghai Univ.,* 1998, **2**, 156–163.
(b) H. Yao, N. Li, S. Xu, J.-Z. Xu, J.-J. Zhu and H.-Y. Chen, *Biosens. Bioelectron.,* 2005, **21**, 372–377.
(c) J. Li, W. Zhu and H. Wang, *Anal. Lett.,* 2009, **42**, 366–380.
(d) I. Tiwari and M. Singh, *Microchim. Acta,* 2011, **174**, 223–230.
(e) Biosensors and modern biospecific analytical techniques, Volume 44 (Comprehensive Analytical Chemistry), ed. L. Gorton, Elsevier, 2005, 635 p.
17. K. M. Gangotri and C. Lal, *Energy Sources,* 2001, **23**, 267–273.
18. A. K. Jana, *J. Photochem. Photobiol., A*, 2000, **132**, 1–17.
19. T. M. Ayers , S. T. Akin, C. J. Dibble and M. A. Duncan, *J. Chem. Educ.,* 2014, **91**, 291–296.
20. J. J. Gaumet and G. Strouse, *Mater. Sci. Eng., C,* 2002, **19**, 299–304.
21. C. A. Schalley and A. Springer, Mass spectrometry of non-covalent complexes: supramolecular chemistry in the gas phase, John Wiley & Sons, 2009, 571 p.
22. (a) G. Pelzer, E. De Pauw, V. D. Dao and J. Marient, *J. Phys. Chem.,* 1984, **88**, 5065–5068.

(b) R. L. Cerny and M. L. Gross, *Anal. Chem.,* 1985, **57**, 1160–1163.
(c) B. D. Musselman and J. T. Watson, *Biomed. Environ. Mass Spectrom.,* 1987, **14**, 247–248.
(d) P. J. Gale, B. L. Bentz, B. T. Chait, F. H. Field and R. J. Cotter, *Anal. Chem.,* 1986, **58**, 1070–1076.
(e) B. L. Bentz and P. J. Gale, *Int. J. Mass Spectrom. Ion Processes.,* 1987, **78**, 115–130.
(f) J. N. Kyranos and P. Vouros, *Biol. Mass Spectrom.,* 1990, **19**, 628–634.
(g) K. Vekey and L. F. Zerilli, *Org. Mass Spectrom.,* 1991, **26**, 939–944.
(h) J. L. Aubagnac, I. Gilles, R. Lazaro, R. M. Claramunt, G. Gosselin and J. Martinez, *Rapid Commun. Mass Spectrom.,* 1995, **9**, 509–511.
(i) P. Cabildo, R. Claramunt, D. Sanz, J. Elguero, C. Enjalbal and J. L. Aubagnac, *Rapid Commun. Mass Spectrom.,* 1996, **10**, 1071–1075.

23. (a) J. Zhang, V. Frankevich, R. Knochenmuss, S. D. Friess and R. Zenobi, *J. Am. Soc. Mass Spectrom.,* 2003, **14**, 42–50.
(b) Y. Itoh, Y. Ohashi, T. Shibue, A. Hayashi, S. Maki, T. Hirano and H. Niwa, *J. Mass Spectrom. Soc. Jpn.,* 2002, **50**, 52–57.
(c) Y. Ohashi and Y. Itoh, *Curr. Org. Chem.,* 2003, **7**, 1605–1611.

24. S. Okuno, M. Nakano, G. E. Matsubayashi, R. Arakawa and Y. Wada, *Rapid Commun. Mass Spectrom.,* 2004, **18**, 2811–2817.

25. D. Asakawa and K. Hiraoka, *J. Mass Spectrom.,* 2009, **44**, 461–465.

26. (a) D. J. Burinsky, R. L. Dilliplane, G. C. DiDonato and K. L. Busch, *Org. Mass Spectrom.,* 1988, **23**, 231–235.
(b) C. W. Kazakoff and R. T. B. Rye, *Org. Mass Spectrom.,* 1991, **26**, 154–156.

27. M. V. Kosevich, V. V. Chagovets, I. V. Shmigol, S. V. Snegir, O. A. Boryak, V.V. Orlov, V. S. Shelkovsky, V. A. Pokrovskiy and A. Gomory, *J. Mass Spectrom.,* 2008, **43**, 1402–1412.

28. M. V. Kosevich, O. A. Boryak, V. V. Orlov, V. S. Shelkovsky, V. V. Chagovets, S. G. Stepanian, V. A. Karachevtsev and L. Adamowisz, *J. Mass Spectrom.,* 2006, **41**, 113–123.

29. V. S. Shelkovskii, M. V. Kosevich, V. V. Chagovets, O. A. Boryak, V. V. Orlov, S. V. Snegir', I. V. Shmigol' and V. A. Pokrovskii, *J. Anal. Chem.,* 2010, **65**, 1388–1396.

30. T. V. Fesenko, M. V. Kosevich, N. I. Surovtseva, V. A. Pokrovskiy, A. M. Eremenko and N. P. Smirnova, *Mass-Spectrometria*. 2007, **4**, 289–296.

31. I. V. Shmigol, S. A. Alekseev, O. Yu. Lavrynenko, N. S. Vasylieva, V. N. Zaitsev, D. Barbier and V. A. Pokrovsky, *J. Mass Spectrom.,* 2009, **44**, 1234–1240.

32. V. V. Chagovets, M. V. Kosevich, S. G. Stepanian, O. A. Boryak, V. S. Shelkovsky, V. V. Orlov, V. S. Leontiev, V. A. Pokrovskiy, L. Adamowicz and V.A. Karachevtsev, *J. Phys. Chem. C*, 2012, **116**, 20579−20590.

33. A. Benninghoven, *Int. J. Mass Spectrom. Ion Phys*., 1983, **53**, 85–99.

34. (a) W. V. Ligon and S. B. Dorn, *Int. J. Mass Spectrom. Ion Proc.,* 1984, **57**, 75–90.
(b) W. V. Ligon and S. B. Dorn, *Int. J. Mass Spectrom. Ion Proc.,* 1987, **78**, 99–113.

35. P. A. Lyon, W. L. Stebbings, F. W. Crow, K. B. Tomer, D. L. Lippstreu and M. L. Gross, *Anal. Chem.,* 1984, **56**, 8–13.

36. L. Ceraulo, G. Giorgi, V. Turco Liveri, D. Bongiorno, S. Indelicato, F. Di Gaudio and S. Indelicato, *Eur. J. Mass Spectrom.,* 2011, **17**, 525–541.

37. M. V. Kosevich, V. V. Chagovets, V. S. Shelkovsky, O. A. Boryak, V. V. Orlov, A. Gomory and P. Vegh, *Rapid Commun. Mass Spectrom.*, 2007, **21**, 466–478.
38. Electrospray and MALDI mass spectrometry: fundamentals, instrumentation, practicalities, and biological applications. 2nd ed., ed. R. Cole, John Wiley & Sons, 2010, 896 p.
39. MALDI MS: A practical guide to instrumentation, methods, and applications, 2-nd Ed., ed. F. Hillenkamp, J. Peter-Katalinic, Wiley-Blackwell, 2013, 480 p.
40. A. Benninghoven, F. G. Rudenauer and H. W. Werner, Secondary ion mass spectrometry: basic concepts, instrumental aspects, applications and trends, Wiley, 1987, 1264 p.
41. V. Cherepin, Secondary ion mass spectroscopy of solid surfaces, VNU Science Press, 1987, 141 p.
42. V. A. Pashynskaya, M. V. Kosevich, A. Gomory, O. V. Vashchenko and L. N. Lisetski, *Rapid Commun. Mass Spectrom.,* 2002, **16**, 1706–1713.
43. M. V. Kosevich, V. S. Shelkovsky, O. A. Boryak and V. V. Orlov, *Rapid Commun. Mass Spectrom.,* 2003, **17**, 1781–1792.
44. I. Bhattacharyya, J. T. Maze, G. E. Ewing and M. F. Jarrold, *J. Phys. Chem. A,* 2011, **115**, 5723–5728.
45. J. Wei, J. M. Buriak and G. Siuzdak, *Nature*, 1999, **399**, 243–246.
46. W. G. Lewis, Z. Shen, M. G. Finn and G. Siuzdak, *Int. J. Mass Spectrom.,* 2003, **226**, 107–116.
47. A. Dominguez, A. Fernandez, N. Gonzalez, E. Iglesias and L. Montenegro, *J. Chem. Educ.,* 1997, **74**, 1227–1231.
48. S. Mery, S. A. Alekseev, V. N. Zaitsev and D. Barbier, *Sens. Actuators, B*, 2007, **126**, 120–125.
49. R. Knochenmuss and R. Zenobi, *Chem. Rev.,* 2003, **103**, 441–452.
50. V. E. Frankevich, J. Zhang, S. D. Friess, M. Dashtiev and R. Zenobi, *Anal. Chem.,* 2003, **75**, 6063–6067.
51. H. Hachisako, Y. Motozato, R. Murakami and K. Yamada, *Chem. Lett.,* 1992, **21**, 219–222.
52. T. M. Ryan , R. J. Day and R. G. Cooks, *Anal. Chem.,* 1980, **52**, 2054–2057.
53. V. A. Pashynska, M. V. Kosevich, A. Gomory, Z. Szilagyu, K. Vekey and S. G. Stepanian, *Rapid Commun. Mass Spectrom.,* 2005, **19**, 785–797.
54. (a) A. Tani, A. J. Thomson and J. N. Butt, *Analyst*, 2001, **126**, 1756–1759.
(b) J. Y. Gu, X. J. Lu and H. X. Ju, *Electroanalysis,* 2002, **14**, 949–954.
(c) D. Pan, X. Zuo, Y. Wan, L. Wang, J. Zhang, S. Song and C. Fan, *Sensors,* 2007, 7, 2671–2680.
55. (a) M. N. Usacheva, M. C. Teichert and M. A. Biel, *J. Photochem. Photobiol. B*, 2003, **71**, 87–98.
(b) M. N. Usacheva, M. C. Teichert and M. A. Biel, *Lasers Surg. Med.*, 2003, **33**, 311–319.
56. E. Morgounova, Q. Shao, B. J. Hackel, D. D. Thomas and S. Ashkenazi, *J. Biomed. Opt.,* 2013, **18**, 056004-1–056004-8.
57. H. Hachisako, Y. Motozato, R. Murakami and K. Yamada, *Chem. Lett.,* 1992, **21**, 219–222.
58. D. B. Tada, L. M. Rossi, C. A. P. Leite, R. Itri and M. S. Baptista, *J. Nanosci. Nanotechnol.*, 2010, **10**, 3100-3108.
59. S. G. Boxer, M. L. Kraft and P. K. Weber, *Annu. Rev. Biophys.*, 2009, **38**, 53–74.
60. L. A. McDonnell and R. M. A. Heeren, *Mass Spectrom. Rev.,* 2007, **26**, 606–643.

61. J. Pól, M. Strohalm, V. Havlíček and M. Volný, *Histochem. Cell Biol.,* 2010, **134**, 423–443.
62. E. M. Weaver and A. B. Hummon, *Adv. Drug Delivery Rev*., 2013, **65**, 1039–1055.
63. R. L. Caldwell and R. M. Caprioli, *Mol. Cell. Proteomics.,* 2005, **4**, 394–401.

Figure Captions

Fig. 1. Schematic representation of (SDS + MB) system at the liquid-gas interface:
a) double electric layer formed by SDS anions and Na^+ counterions with inclusion of $2MB^{2+}$ dimer; b) orthogonal view of arrangement the SO_3^- polar heads of SDS with adsorbed MB^+ cation. (Colour scheme for atoms: hydrogen – white, carbon – grey or dark grey, nitrogen – blue, oxygen – red, sulfur – yellow, chlorine – green, sodium – magenta.)

Fig. 2. FAB mass spectra of the surface layer of (SDS + MB) system in glycerol matrix:
a) pure MB (10^{-2} M) without SDS;
b) a mixture of 10^{-1} M SDS and 10^{-2} M MB;
c) a mixture of 10^{-1} M SDS and 10^{-4} M MB.

Fig. 3. LDI mass spectra of MB and (SDS + MB) systems: a) pure crystalline MB; b) a mixture of 10^{-2} M MB and 10^{-1} M SDS; c) a mixture of 10^{-4} M MB and 10^{-1} M SDS; d) LDI (DIOS) of MB adsorbed on PS-SO_3^- ion-exchange surface.